scientific reports

Check for updates

OPEN

Protective effect of tanshinone IIA against *Listeria monocytogenes* infection in vitro and in vivo

Haiting Wang[1,2], Sangyu Hu[3], Haihua Feng[3] & Hongxiang Sun[2]✉

Listeriolysin O (LLO) is a vital virulence factor for the intracellular replication and pathogenesis of *Listeria monocytogenes*. The search for an effective LLO activity inhibitor as an alternative approach for the treatment of *L. monocytogenes* infection has attracted great attention. Tanshinone IIA (Tan IIA) is a bioactive compound in the traditional Chinese medicine "Danshen". In this study, the protective effect of Tan IIA against *L. monocytogenes* infection was investigated using hemolysis test, LDH release method, oligomerization assay and molecular dynamics simulation in combination with in vivo mouse experiment. Tan IIA significantly inhibited the pore-forming activity of LLO by forming a stable LLO – Tan IIA complex. Meanwhile, Tan IIA concentration-dependently decreased the cytotoxicity of *L. monocytogenes* toward J774 and BeWo cells with the inhibitory rates being 41.3% and 54.5% at concentration of 8 μg/mL, respectively. Furthermore, the intracellular growth of *L. monocytogenes* was also inhibited by Tan IIA in an LLO-dependent manner. Of note, Tan IIA (80 mg/kg) protected mice against *L. monocytogenes* infections with the increased survival rate of 26.7%, reduced bacterial loads, alleviated tissue damages, and diminished inflammation. In conclusion, Tan IIA might be a promising anti-virulence candidate for the treatment of L. *monocytogenes* infection.

Keywords Tanshinone IIA, Listeriolysin O, *Listeria monocytogenes*, Anti-virulence

Abbreviations

CDC	Cholesterol-dependent cytolysin
CFU	Colony forming unit
DMEM	Dulbecco's modified Eagle medium
DMSO	Dimethylsulfoxide
ECL	Enhanced chemiluminescence
ELISA	Enzyme-linked immunosorbent assay
FBS	Fetal bovine serum
H&E	Hematoxylin and eosin
HRP	Horseradish reroxidase
ICDH	Isocitrate dehydrogenase
IL-6	Interleukin-6
LDH	Lactate dehydrogenase
LLO	Listeriolysin O
MD	Molecular dynamics
MOI	Multiplicity of infection
OD	Optical density
RBC	Red blood cell
Rg	Radius of gyration
RMSD	Root mean square deviation
RMSF	Root mean square fluctuation
SPF	Specific pathogen-free
Tan IIA	Tanshinone IIA

[1]Shandong Provincial Key Laboratory of Livestock and Poultry Breeding, Institute of Poultry Science, Shandong Academy of Agricultural Sciences, Jinan 250100, China. [2]MOA Key Laboratory of Animal Virology, College of Animal Sciences, Zhejiang University, Hangzhou 310058, China. [3]State Key Laboratory for Diagnosis and Treatment of Severe Zoonotic Infectious Diseases, Key Laboratory for Zoonosis Research of the Ministry of Education, Institute of Zoonosis, and College of Veterinary Medicine, Jilin University, Changchun 130062, China. ✉email: sunhx@zju.edu.cn

TNF-α	Tumor necrosis factor-alpha
TSB	Trypticase soy broth
WT	Wide-type

Background

Listeria monocytogenes is a ubiquitous Gram-positive intracellular bacterial pathogen in nature that has been implicated in foodborne illness[1]. *L. monocytogenes* causes a broad range of acute infections including gastroenteritis, sepsis, meningitis, miscarriage, and stillbirth, especially in newborns, the elderly, pregnant women, and immunocompromised patients[2,3]. *L. monocytogenes* poses food safety challenges and threatens human health due to its ability to persist in processing environments, resist refrigeration, and form biofilms[4].

Antibiotic therapy remains the primary strategy for the treatment of listeriosis in clinic. However, the emergence of multidrug-resistant *L. monocytogenes* has increasingly caused global concern in recent years. *L. monocytogenes* exhibits resistance to the antibiotics such as cephalosporin, ciprofloxacin, and tetracycline[5,6]. Therefore, there is an urgent need for new therapeutic approaches to overcome the antibiotic resistance of *L. monocytogenes*. Anti-virulence strategy targeting the virulence factors of pathogenic bacteria may be an alternative method for conventional antibiotic therapy.

Listeriolysin O (LLO), an essential determinant of *L. monocytogenes* pathogenesis, facilitates bacterial internalization and vacuolar escape, resulting in the translocation and intracellular spread of bacteria[7]. LLO has been reported to be a reliable therapeutic target against listeriosis. Some natural compounds such as atractylodin[8] baicalein[9] fisetin[10] genistin[11] and phloretin[12] were reported to inhibit the pore-forming activity activities of LLO in *L. monocytogenes*.

Tanshinone IIA (Tan IIA, Fig. 1A), a bioactive compound in traditional Chinese medicine "Danshen" (the root of *Salvia miltiorrhiza* Bunge; family Lamiaceae), has been widely used to treat cardiovascular and inflammatory diseases in clinic[13]. Tan IIA has been found to possess the anti-atherosclerotic[14–16] antitumor[17–20] anti-inflammatory[21–23] anti-platelet[24] antifibrosis[25] and antioxidative[26] pharmacological effects. In the previous work, in light of the critical role of LLO in *L. monocytogenes* pathogenesis, LLO-targeted biochemical screening was conducted and Tan IIA was found to be an effective blocker of LLO activity.

In the present study, the protective effect of Tan IIA against *L. monocytogenes* infections in vitro and in vivo was investigated and the its mechanisms were explored. This study provides the evidences for Tan IIA as a promising anti-virulence candidate for the treatment of listeriosis.

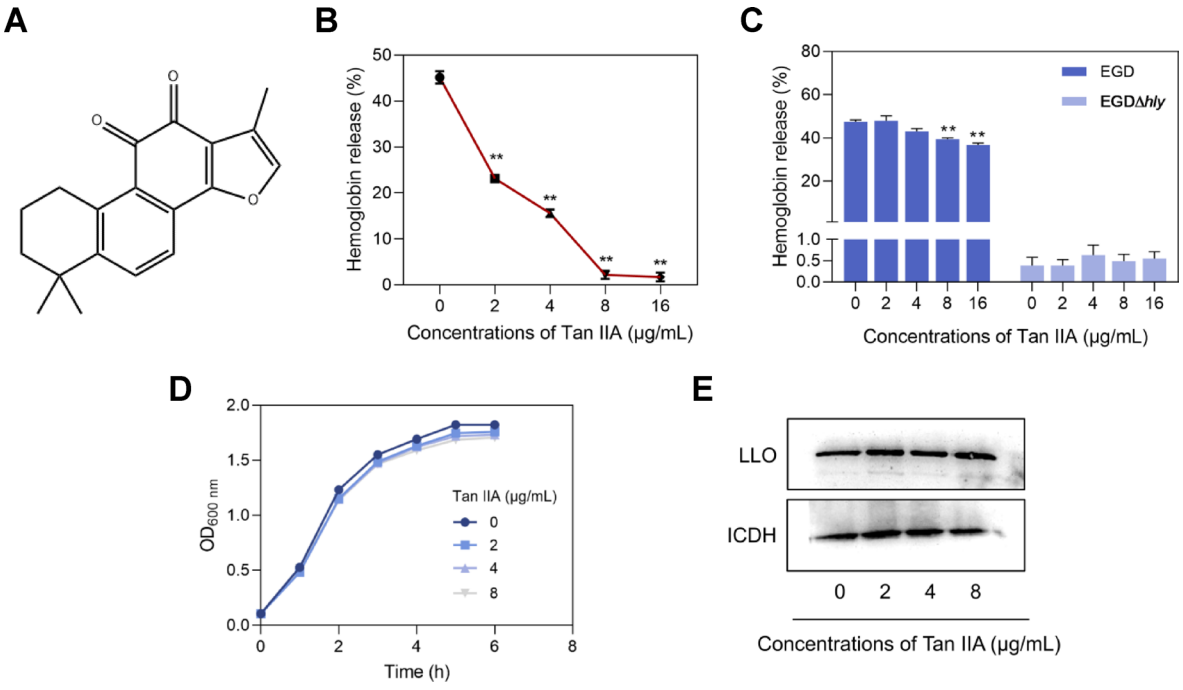

Fig. 1. Tan IIA suppressed the pore-forming property of LLO. (**A**) Chemical structure of tanshinone IIA (Tan IIA). (**B**, **C**) Inhibitory effects of Tan IIA on the hemolysis of rabbit red blood cell suspension induced by LLO (**B**) and the cultures of *L. monocytogenes* wide-type EGD and LLO-deficient mutant EGDΔ*hly* strains (**C**). Phosphate buffered saline (PBS) and distilled water were included as negative and positive haemolytic controls, respectively. The data were presented as means ± SD ($n = 3$). $^{**}p < 0.01$ vs. 0 μg/mL. (**D**) The growth curve of *L. monocytogenes* treated with Tan IIA (0–8 μg/mL). (**E**) The protein expression levels of LLO and isocitrate dehydrogenase (ICDH) in *L. monocytogenes* treated with Tan IIA (0–8 μg/mL) *via* Western blotting. The figure shown is representative of three independent experiments.

Results

Tan IIA inhibited the pore-forming activity of LLO by disrupting oligomerization

In light of the important roles of LLO in the *L. monocytogenes* pathogenesis, the effect of Tan IIA on the pore-forming activity of secreted LLO was detected using the hemolytic test. Tan IIA significantly decreased the hemolytic activity of LLO (Fig. 1B) and the cultures of *L. monocytogenes* wide-type (WT) EGD strain (Fig. 1C) toward 2.5% rabbit red blood cell (RBC) suspension at the concentration ranging from 2 to 16 μg/mL. However, *L. monocytogenes* LLO-deficient mutant EGDΔ*hly* strain treated with and without Tan IIA at the concentration of 2–16 μg/mL did not exhibit significant hemolytic activity on rabbit RBC. To explore whether the decreased hemolytic activity of Tan IIA was associated with its inhibition of bacterial survival, the growth curve of *L. monocytogenes* in the presence or absence of Tan IIA was detected. As shown in Fig. 1D, Tan IIA at the concentrations of 2, 4, and 8 μg/mL had no significant influence on bacteria growth, suggesting that the inhibitory effects of Tan IIA on the LLO-mediated hemolytic activity was not due to its antimicrobial activity.

To clarify the mechanisms of the inhibitory action of Tan IIA on the hemolytic activities of LLO, the LLO protein expression levels in *L. monocytogenes* was determined by western blotting. The results showed that Tan IIA had no visible effect on the protein expression of LLO in *L. monocytogenes* (Fig. 1E). These results indicated that Tan IIA inhibited the haemolytic activity of LLO not by regulating LLO protein expression.

LLO oligomerizes and forms pre-pore complexes in cholesterol-structure lipid membranes of host cells[27,7]. The oligomerization was further analyzed to visualize LLO oligomers and monomers by Western blot assays. Tan IIA at the concentrations of 2, 4, and 8 μg/mL significantly blocked the LLO monomers to oligomerize into a high molecular weight (MW) complex, as evidenced by the decreased oligomer/monomer optical density ratio (Fig. 2A, B). These results suggested that Tan IIA suppressed the hemolytic activity of LLO through inhibiting its oligomerization.

Identification of the binding residues of LLO with Tan IIA

To predict the binding sites of LLO and Tan IIA, molecular dynamics simulation was conducted, and the potential interactions between Tan IIA and LLO was shown in Fig. 3A. The radius of gyration (Rg) indicated the structural equilibrium of the LLO – Tan IIA system (Fig. 3B). The root mean square fluctuation (RMSF) and root mean square deviation (RMSD) revealed the stability of LLO – Tan IIA complex (Fig. 3C, D). Importantly, Tan IIA was attached to the active residue GLU446, TYR440, VAL100, ASN473, LEU503, ALA474, and GLY472 via *van der Waals* interactions, as well as PRO502 and VAL438 residues participated in Alkyl interactions, and TYR414 and ARG475 participated in Pi-Pi stacked and Pi-Alkyl interactions, respectively (Fig. 3E). The energy decomposition of key amino acid residues was shown in Fig. 3F. These findings suggested that interactions of Tan IIA and LLO formed the complex to inhibit the pore-forming activity of LLO.

Tan IIA inhibited *L. monocytogenes*-infected cytotoxicity and intracellular survival in J774 and bewo cells

LLO forms pores in cholesterol-enriched membranes to trigger host cell death. Tan IIA showed no significant cytotoxicity against the J774 and BeWo cells at the concentrations ranging from 2 to 16 μg/mL (Fig. 4A, B). However, Tan IIA concentration-dependently significantly inhibited the cytotoxicity of *L. monocytogenes* toward J774 and BeWo cells at the concentrations of 2–8 μg/mL, as evidenced by a decreased lactate dehydrogenase (LDH) release (Fig. 4C, D). Meanwhile, live/dead staining of J774 cells infected with *L. monocytogenes* indicated

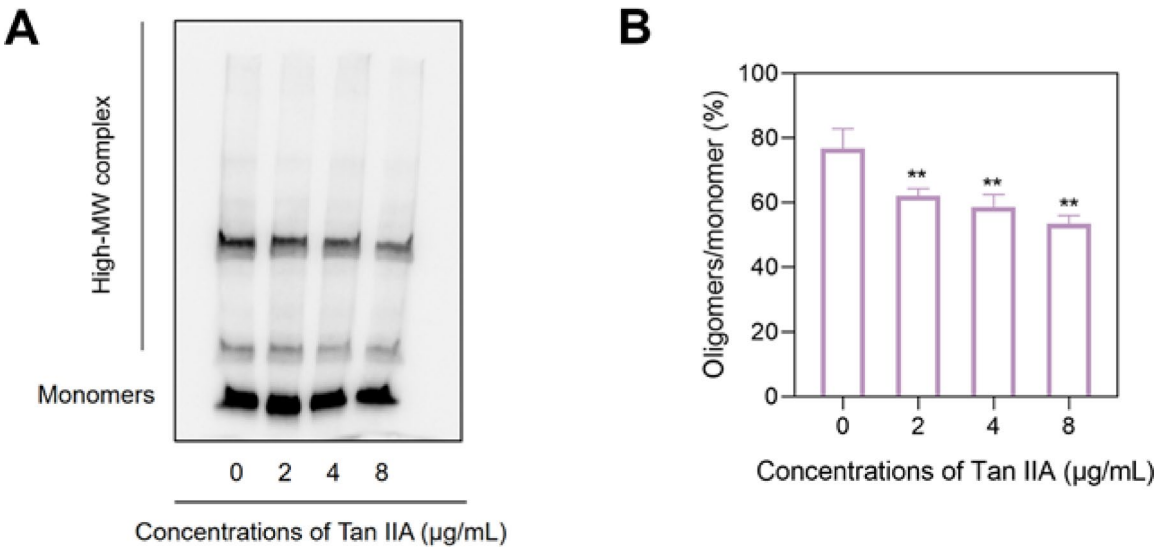

Fig. 2. Tan IIA blocked the oligomerization of LLO. (**A**, **B**) The oligomerization of LLO treated with Tan IIA (0–8 μg/mL) using western blotting. The figure (**A**) shown is representative of three independent experiments. The data (**B**) are expressed as means ± SD ($n = 3$). $^{**}p < 0.01$ vs. 0 μg/mL.

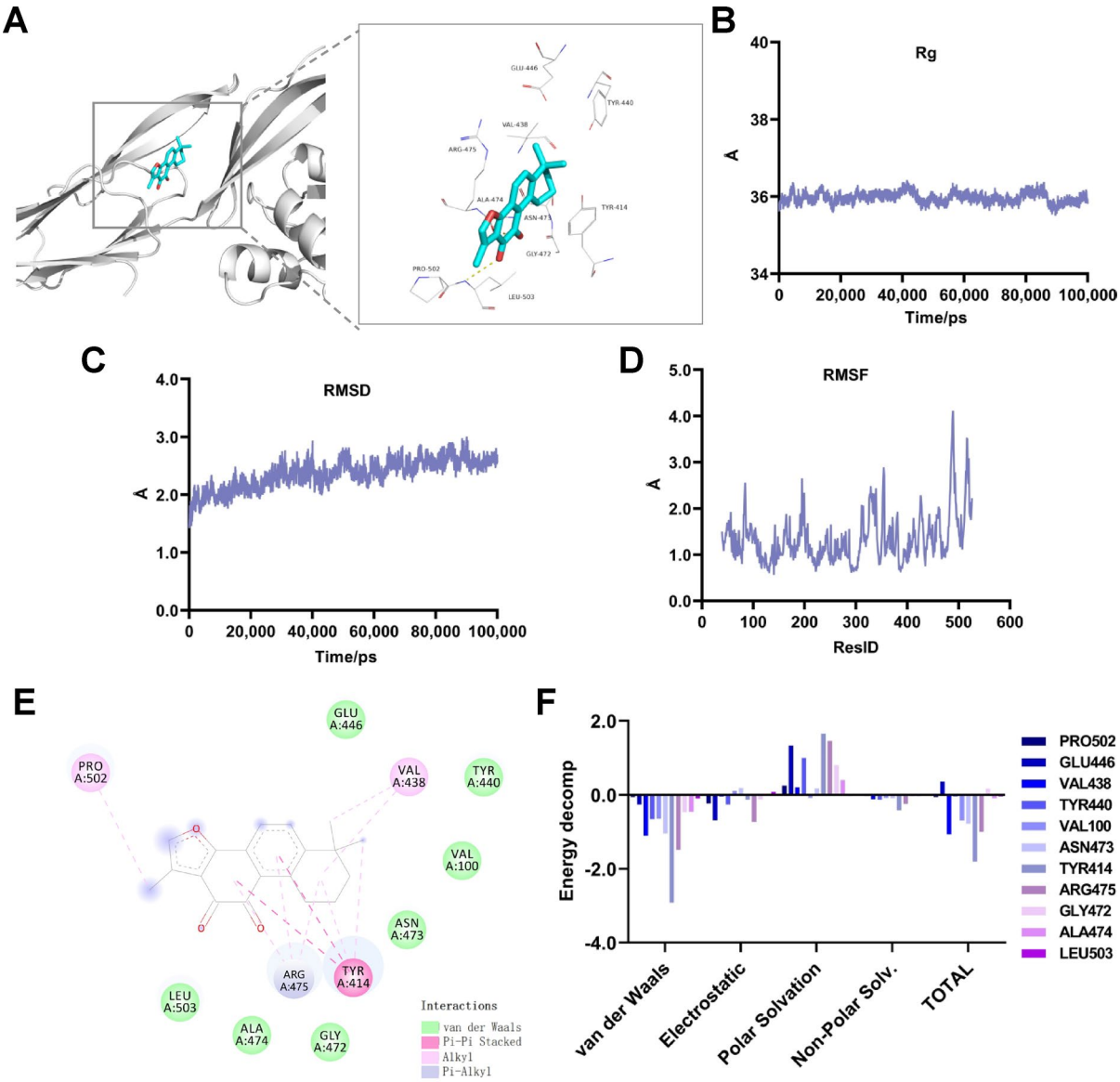

Fig. 3. The binding residues of Tan IIA–LLO complex. (**A**) The binding mode between Tan IIA and LLO was identified using molecular dynamics simulation. (**B**–**D**) The radius of gyration (Rg), root mean square deviation (RMSD) and root mean square fluctuation (RMSF). (**E**) The predicted binding mode of Tan IIA–LLO complex. (**F**) The energy decomposition of the binding residues.

that the dead cells stained with ethidium homodimer-1 (red fluorescent dye) were decreased by Tan IIA at the concentration of 4 and 8 μg/mL (Fig. 4E).

LLO mediates the escape of *L. monocytogenes* and its replication in the cytoplasm[28]. As shown in Fig. 4F, LLO-producing *L. monocytogenes* wild-type EGD strain harbored the potent intracellular replication capacity, however which was suppressed in *hly*-deficient mutant (EGDΔ*hly*). Notably, Tan IIA (4 μg/mL) significantly inhibited the intracellular growth of *L. monocytogenes* in J774 cells (Fig. 4F). In addition, Tan IIA could significantly reduce the intracellular loads of *L. monocytogenes* wild-type EGD and *hly* complementation EGDΔ*hly*::*hly* strains in BeWo cells, but not affect that of *hly*-deficient mutant EGDΔ*hly* strain (Fig. 4G). Collectively, these findings indicated that Tan IIA significantly attenuated *L. monocytogenes* pathogenicity in vitro in the LLO-dependent manner.

Tan IIA protected from *L. monocytogenes* infection in mice

The therapeutic potency of Tan IIA on the *L. monocytogenes* infection in mice was investigated. As shown in Fig. 5A, the oral administration of Tan IIA (80 mg/kg) increased the survival rate of EGD-infected mice by 26.7% in comparison with the *L. monocytogenes* EGD-infection group. Consistently, the bacterial loads in liver, spleen, and kidney tissues of *L. monocytogenes*-infected mice were significantly decreased by Tan IIA at the doses

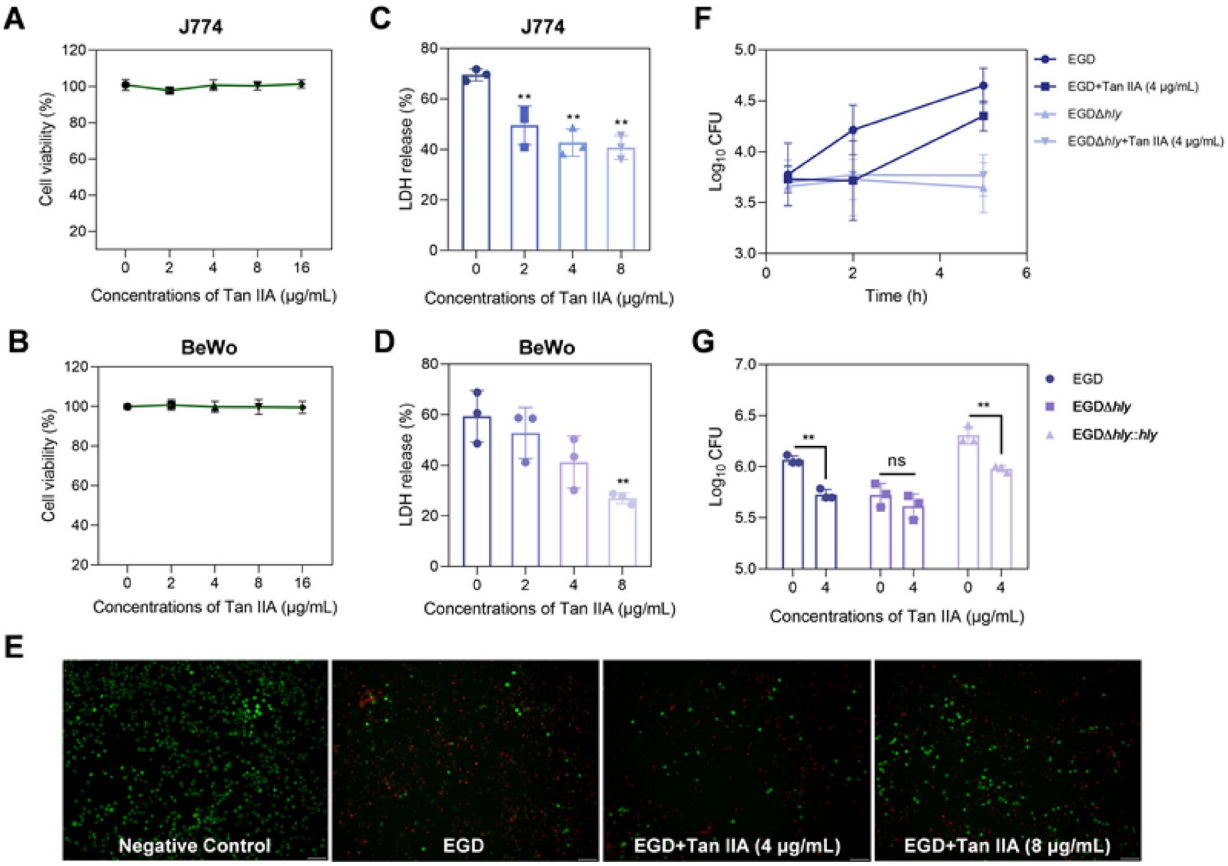

Fig. 4. Tan IIA inhibited *L. monocytogenes*-infected cytotoxicity and intracellular survival in J774 and BeWo Cells. (**A**, **B**) The viabilities of J774 (**A**) and BeWo (**B**) cells treated with Tan IIA at the indicated concentrations *via* the LDH assay. (**C**, **D**) Release of lactate dehydrogenase (LDH) from J774 (**C**) and BeWo (**D**) cells treated with *L. monocytogenes* EGD alone or in combination with Tan IIA (2, 4, and 8 μg/mL). (**E**) The morphological changes of J774 cells treated with *L. monocytogenes* EGD alone or in combination with Tan IIA (4 and 8 μg/mL) using LIVE/DEAD Viability/Cytotoxicity Kit. Live and dead cells were stained into green and red fluorescence by calcein AM and ethidium homodimer-1, respectively. The figure shown is representative of three independent experiments. Scale bars: 50 μm. (**F**) Intracellular bacterial growth in J774 cells infected with wide-type EGD or the *hly* deletion mutant EGDΔ*hly L. monocytogenes* co-cultured with or without Tan IIA (4 μg/mL) using plate counting method. (**G**) The intracellular bacterial loads in the BeWo cells infected with *L. monocytogenes* wide-type EGD, *hly* deletion mutant EGDΔ*hly*, or *hly* complementation EGDΔ*hly*::*hly* strain in the presence or absence of Tan IIA (4 μg/mL) were measured 2 h post-infection by colony counting. The data are expressed as means ± SD ($n = 3$). $^{**}p < 0.01$ vs. 0 μg/mL, ns, not significant.

of 40 and 80 mg/kg as evidenced by approximate 1 log reduction of colony forming unit (CFU) compared with the EGD-infection control group (Fig. 5B).

The hematoxylin and eosin (H&E) staining revealed that *L. monocytogenes* infection induced the marked hemorrhage, congestion, or cell necrosis in liver and spleen tissues, alongside disintegration of the intact structure of renal tubular in kidney tissues in mice (Fig. 5C). Nevertheless, Tan IIA alleviated tissue damages as illustrated by an intact centrilobular portion and renal tubular structure, decreased hemorrhage, congestion, and inflammatory cell recruitment (Fig. 5C). Meanwhile, the levels of pro-inflammatory cytokines IL-6 and TNF-α in the liver homogenates were determined by enzyme-linked immunosorbent assay (ELISA). *L. monocytogenes* infection significantly enhanced the levels of pro-inflammatory cytokines in mouse liver tissues compared with normal control group (Fig. 5D, E). However, the treatment of Tan IIA at dose 80 mg/kg significantly decreased these two pro-inflammatory factor levels in the liver tissues of *L. monocytogenes*-infected mice (Fig. 5D, E). These findings suggested that Tan IIA could protect mice against the *L. monocytogenes* infection.

Discussion

Anti-virulence strategy as an antibiotics alternative therapeutic regimen is currently being developed *via* inhibiting the bacterial virulence as opposed to the killing of pathogenic microbes, and thereof, abrogating the host pro-inflammatory response to microorganisms[10,29]. *L. monocytogenes* implicated in numerous outbreaks and related deaths of listeriosis with high mortality has been reported to secrete multifarious virulence factors, assisting to cross and breach the blood-brain, placental and intestinal barrier[30,31]. Notably, the cholesterol-dependent pore-forming toxin LLO contributes the survival and pathogenicity of *L. monocytogenes via*

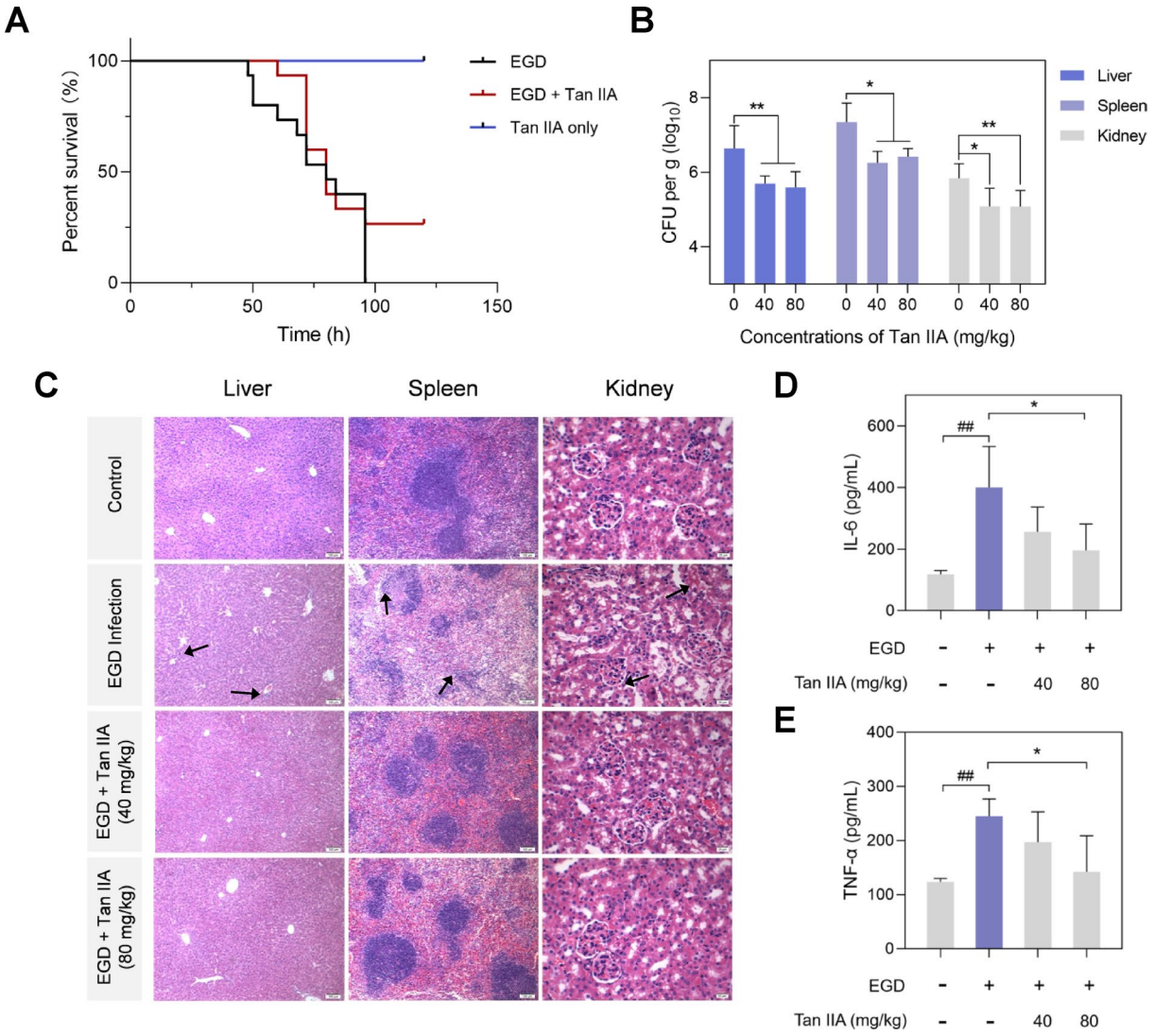

Fig. 5. Tan IIA protected from *L. monocytogenes* infection in mice. (**A**) Survival analysis of *L. monocytogenes*-infected mice treated with or without Tan IIA ($n = 15$). (**B**) The bacterial loads in liver, spleen, and kidney tissues ($n = 6$). (**C**) Histopathological changes of liver, spleen, and kidney tissues. The tissue sections were stained using hematoxylin and eosin (H&E) staining. The light photomicrographs shown were representative of tissue sections from six mice per group. The black arrows showed the congestion in liver tissues, unclear boundary between red and white pulp in spleen tissues, and incomplete glomerular morphology in kidney tissues. Scale bar = 100 or 20 μm. (**D**, **E**) IL-6 and TNF-α levels in the liver homogenates by enzyme-linked immunosorbent assay (ELISA). The data are expressed as means ± SD ($n = 4$). $^{*}P < 0.05$*vs. L. monocytogenes*-infected group; $^{\#\#}P < 0.01$ vs. the vehicle control group.

puncturing the phagosomal membranes and escaping from host cell vacuoles, thereby triggering pathological reactions and inflammation activation[32]. This evidence rendered the cytotoxin LLO as a promising target for the treatment of *L. monocytogenes* infections.

In the previous work, Tan IIA was found to be an effective blocker of LLO activity by LLO-targeted biochemical screening. Tao et al.[33] reported that the oral administration of tanshinone extract (containing 11% Tan IIA and 3% cryptotanshinone) at a dose of 5 g/kg did not cause severe side effects, toxicity, and death in mice. It was also reported that Tan IIA was administered to the gastric cancer AGS cell xenograft tumor-bearing SCID mice at concentrations of 30, 60 and 90 mg/kg by intraperitoneal injection for 8 weeks[34]. Therefore, to excavate a safe, promising and novel anti-virulence therapeutic agent, Tan IIA was evaluated for the protective effect against *L. monocytogenes* infection in vitro and in vivo and its molecular mechanism was also explored.

In this study, Tan IIA was found to block the pore-forming activity of *L. monocytogenes* virulence factor LLO at the concentrations ranging from 2 to 8 μg/mL, thereby suppressing the *L. monocytogenes*-mediated cytotoxicity. LLO, a cholesterol-dependent cytolysin (CDC) secreted by *Listeria monocytogenes*, undergoes stepwise oligomerization to form β-barrel pores. Hence, the inactivation of LLO is mechanistically driven by

the inhibition of oligomerization of LLO, disrupting pore-forming capacity[35]. Tan IIA inhibited the hemolytic activity of LLO through forming Tan IIA-LLO complex to block its oligomerization.

The in vivo data revealed that Tan IIA exerted therapeutic potentials for *L. monocytogenes* infection in mice by attenuating the pathological damage and minimizing the microbial colonization. Tan IIA was reported to possess the anti-inflammatory potentials in atherosclerotic lesion, brain disease, and the *Mycobacterium tuberculosis* infection[17,21–23] as well as the antioxidative effects by activating the Nrf2 signaling pathway[26] supporting its therapeutic potentials for *L. monocytogenes infection*. *L. monocytogenes* disseminates from the gastrointestinal tract to the liver, which leads to the colonization of liver and spleen in guinea pigs[36]. In the mouse model, the overwhelming replication of *L. monocytogenes* in the liver and spleen leads to a secondary bacteremia composed of a combination of cell-free and intracellular bacteria[36]. It was also reported that *L. monocytogenes*-induced Kupffer cell death in the liver appeared as a key signal orchestrating not only type-1 microbicidal inflammation, but also type-2-mediated tissue repair upon infection[37]. Therefore, the levels of TNF-α and IL-6 in liver homogenates were determined in this study. Tan IIA significantly decreased the levels of inflammatory cytokines IL-6 and TNF-α in the liver tissues from *L. monocytogenes*-infected mice, which might also be one of the reasons for its protection against *L. monocytogenes* infection in mice.

Conclusions

In summary, Tan IIA was for the first time demonstrated to protect against *Listeria monocytogenes* infection in vitro and in vivo. Tan IIA inhibited the pore-forming activity of LLO and decreased the cytotoxicity and intracellular multiplication of *L. monocytogenes*. Furthermore, Tan IIA reduced the bacterial loads, alleviated tissue damages, and alleviated inflammatory responses in mice infected with *L. monocytogenes*. Our findings suggested that Tan IIA might be a promising anti-virulence candidate for the treatment of listeriosis. Further research is needed on its safety and clinical trials for target animals.

Methods

Materials and reagents

Trypticase soy broth (TSB) was purchased from Qingdao Hope Biol-Technology Co., Ltd., Qingdao, China. Fetal bovine serum (FBS) was purchased from Biological Industries Biological Industries Ltd., Kibbutz Beit Haemek, Israel. High glucose Dulbecco's modified Eagle medium (DMEM) and Ham's F12K media were obtained from Corning, NY, USA. LDH cytotoxicity assay kit was acquired from Roche, Basel, Switzerland. LIVE/DEAD™ viability/cytotoxicity kit was acquired from Invitrogen, Carlsbad, CA, USA. Anti-rabbit listeriolysin (LLO) polyclonal antibody (ab200538) and horseradish peroxidase (HRP)-conjugated goat anti-rabbit IgG H&L (ab205718) were acquired from Abcam, Cambridge, UK. HRP-conjugated mouse anti-His-Tag antibody was acquired from ABclonal Technology Co., Ltd., Wuhan, China. Enhanced chemiluminescence (ECL) kit was acquired from Beyotime, Shanghai, China. Mouse IL-6 and TNF-α ELISA kits were obtained from BioLegend, Beijing, China. Anti-rabbit isocitrate dehydrogenase (ICDH) polyclonal antibody (ABS2090) and dimethylsulfoxide (DMSO) were acquired from Sigma-Aldrich, St. Louis, MI, USA.

The tanshinone IIA (analytical grade, ≥98%, Fig. 1A) was purchased from Ruifensi Biotechnology Co., Ltd., Chengdu, China. The stock solution in DMSO was diluted into the desired concentration with the cell culture medium. The final concentration of DMSO in all experiments was less than 0.1% and did not show any detectable effect on cell growth and bacteria.

Bacterial strains and culture

L. monocytogenes wide-type EGD strain, LLO deletion mutant EGDΔ*hly*, and LLO complementation strain EGDΔ*hly*::*hly* were kindly provided by Dr. Masao Mitsuyama (Department of Microbiology, Kyoto University Graduate School of Medicine, Japan). Bacteria were grown to the logarithmic growth phase in TSB medium at 37 °C with continuous shaking at 200 rpm.

Cell lines and culture

The mouse J774 macrophages and human placental choriocarcinoma BeWo cells were obtained from the European National Collection of Authenticated Cell Cultures (ECACC), UK Health Security Agency. J774 and BeWo cells were maintained in the logarithmic phase of growth in high glucose DMEM medium and F12K medium Supplemented with 10% heat-inactivated FBS, 100 IU/mL penicillin, and 100 μg/mL streptomycin in an incubator at 37 °C with 5.0% CO_2 atmosphere, respectively. Cell line identity was validated through short tandem repeat profiling, and routine mycoplasma testing was negative for contamination.

Hemolysis assay

The recombinant LLO, EGD, or EGDΔ*hly* culture supernatants were diluted with phosphate buffered saline (PBS, 35 mM Na_3PO_4, 125 mM NaCl, pH 5.5), and then were incubated with different concentrations of Tan IIA (0, 2, 4, 8, and16 μg/mL) at 37 °C for 30 min. Subsequently, the samples were incubated with 2.5% rabbit RBC suspension for 15 min. The supernatant of the mixtures was harvested (10,000 rpm, 2 min) and the absorbance values were monitored at 570 nm using a Microplate Reader (BioTek, synergy LX, Winooski, VT, USA). PBS and distilled water were included as negative and positive haemolytic controls, respectively. The percentage of lysed RBCs was determined by comparing each sample with distilled water, which was considered 100% hemolysis[38].

Growth curve assay

The growth kinetics of *L. monocytogenes* EGD strain were determined by the spectrophotometric method as described previously[9]. *L. monocytogenes* in logarithmic growth was treated with Tan IIA at the concentrations of

0, 2, 4, and 8 μg/mL. The optical density (OD) values of bacterial cultures were monitored at 600 nm every hour using a spectrophotometer (Unic, UV-2000, Shanghai, China).

Western blotting

The bacterial cultures treated with Tan IIA (0, 2, 4, and 8 μg/mL) were collected and then centrifuged (10,000 g, 5 min). The equal volumes of supernatants were mixed with 5× SDS-PAGE loading buffer (4 : 1). The mixture was boiled 100 °C for 10 min. The denatured proteins were separated on a 12% SDS-polyacrylamide gel *via* electrophoresis, and then transferred onto polyvinylidene fluoride (PVDF) membranes. After blocking the membrane with 5% skim milk in Tris-buffered saline containing 0.1% Tween-20 (TBST) for 2 h at room temperature, the membranes were incubated with the anti-rabbit LLO polyclonal antibody (diluted with blocking buffer at 1 : 1000) or anti-rabbit ICDH polyclonal antibody (diluted with blocking buffer at 1 : 10,000) overnight at 4 °C. Subsequently, the membranes were washed with TBST and incubated with HRP-conjugated goat anti-rabbit IgG H&L for 1 h. After being washed with TBST for three times, the membrane was visualized with the ECL kit on the iBright™ CL1500 Imaging System (Thermo Fisher Scientific, Waltham, MA, USA).

Oligomerization assay

Recombinant LLO was incubated with various concentrations of Tan IIA (0, 2, 4, and 8 μg/mL) at 37 °C for 30 min, and mixed with KCl for an additional 10 min to induce LLO oligomerization. Then, 0.5% rabbit RBC suspension was added and incubated for 10 min. Samples supplemented with 5 × nonreducing loading buffer were heated at 55 °C for 10 min. Then the oligomerization analysis was detected using HRP-conjugated mouse anti-His-Tag antibody by the aforementioned western blotting[38].

Molecular dynamics simulation

The molecular dynamics simulation was performed to analyze the interactions between Tan IIA and LLO using the AMBER 18 software. The crystal structure of LLO protein (PDB ID: 4CDB) was originated from the Research Collaboratory for Structural Bioinformation (RCSB) Protein Data Bank (PDB). The 2D structure of Tan IIA as the molecular docking ligand was obtained from PubChem (https://pubchem.ncbi.nlm.nih.gov/). The molecular dynamics (MD) of LLO – Tan IIA complex was analyzed as the following steps including energy minimization, heating, equilibrant and then dynamics simulation. Finally, the binding free energy between the ligand and protein was calculated using the MM-PBSA method[39,40].

Cytotoxicity and cell viability assay

J774 and BeWo cells infected with or without EGD were incubated with diverse concentrations of Tan IIA for 6 h, and culture supernatants were harvested to measure the levels of lactate dehydrogenase (LDH) using a cytotoxicity detection kit. The cultured J774 cells were then stained with calcein-AM (live cells) and ethidium homodimer-1 (dead cells) using a LIVE/DEAD™ Viability/Cytotoxicity Kit and visualized on an Olympus CKX53 microscope (Olympus, Tokyo, Japan).

Intracellular growth assay

J774 cells (3×10^5 cells/well) in the presence or absence of Tan IIA (4 μg/mL) were infected with EGD or EGDΔ*hly* (MOI = 5) for 30 min. Then, the extracellular bacteria were killed by the addition of 20 μg/ml gentamicin and the cultured cells were washed and lysed for intracellular bacterial counting at the indicated time points.

BeWo cells (3×10^5 cells/well) were seeded into 24-well plates overnight. Cells were incubated with or without Tan IIA (4 μg/mL) following by infection with EGD, EGDΔ*hly* or EGDΔ*hly*::*hly* (MOI = 10). The cells were lysed 2 h post-infection and the intracellular bacterial loads were plated onto the TSB agar plates for microorganisms counting.

Experimental animal, grouping and drug administration

Female BALB/c mice aged 6–8 weeks were purchased from Liaoning Changsheng Biotechnology Co., Ltd. (Liaoning, China). The mice were housed with free access to food and water and acclimated for 1 week before experiments in a specific pathogen-free (SPF) environment. All the procedures were in strict accordance with the China legislation on the use and care of laboratory animals and with the guidelines established by Institute for Experimental Animals of Jilin University. The experimental animal facility and procedures were approved by the Institutional Animal Care and Use Committee of Jilin University. Meanwhile, the study was reported in accordance with ARRIVE guidelines (https://arriveguidelines.org).

For the survival rate analysis, mice were infected with EGD cultures (1×10^7 CFU) via intraperitoneal injection and randomly grouped ($n = 15$ per group). Simultaneously, mice were treated with Tan IIA (80 mg/kg/day) dissolved in the 0.5% sodium carboxymethylcellulose (CMC) *via* oral administration at 12-h intervals.

Additionally, for the bacterial loading analysis, EGD (1×10^6 CFU)-infected mice were randomly divided into 3 groups: Infection control, Tan IIA (40 mg/kg/day) and Tan IIA (80 mg/kg/day) treatment groups, as described above. At 48 h post-infection, the mice were euthanized in a chamber with carbon dioxide and then sacrificed by cervical dislocation. The liver, spleen, and kidney tissue samples were aseptically collected, and then homogenized in ice-cold 9-fold PBS to make 10% homogenates for bacterial load detection and ELISA. And these tissues were fixed in 4% paraformaldehyde for histopathological studies.

Enzyme-linked immunosorbent assay (ELISA)

The 10% liver tissue homogenate was used for measuring the contents of inflammatory cytokines TNF-α and IL-6 by ELISA kits according to the manufacturer's instructions. And the absorbance values in different samples were measured at 450 nm using a Microplate Reader (BioTek, synergy LX, Winooski, VT, USA).

Histopathology observation

The liver, spleen, and kidney tissues fixed with 4% paraformaldehyde were dehydrated through a series of graded ethanol, hyalinized with xylene, embedded in paraffin, and sectioned at 5–μm thicknesses. Microsections were stained using H&E. The histological changes were observed on an Olympus CKX53 microscope (Olympus, Tokyo, Japan).

Statistical analysis

Data were expressed as the means ± SD and examined for their statistically significant differences with the analysis of variance (ANOVA) and Student's *t*-test. The *p*-values of less than 0.05 were statistically significant. The calculations and graphs were performed using GraphPad Prism 9.0 software (GraphPad Software, San Diego, CA, USA).

Data availability

The data would be available from the corresponding author upon reasonable request.

Received: 16 May 2025; Accepted: 11 September 2025
Published online: 15 October 2025

References

1. Manqele, A. et al. Virulence potential and antimicrobial resistance of *Listeria monocytogenes* isolates obtained from beef and beef-based products Deciphered using whole-genome sequencing. *Microorganisms* **12**, 1166 (2024).
2. Li, W. W. et al. The epidemiology of *Listeria monocytogenes* in China. *Foodborne Pathog Dis.* **15** (8), 459–466 (2018).
3. Fotopoulou, E. T., Jenkins, C., Painset, A. & Amar, C. *Listeria monocytogenes*: the silent assassin. *J. Med. Microbiol.* **73**, 001800 (2024).
4. Silva, A. et al. *Listeria monocytogenes* from food products and food associated environments: antimicrobial resistance, genetic clustering and biofilm insights. *Antibiotics* **13** (5), 447 (2024).
5. Wilson, A., Gray, J., Chandry, P. S. & Fox, E. M. Phenotypic and genotypic analysis of antimicrobial resistance among *Listeria monocytogenes* isolated from Australian food production chains. *Genes* **9** (2), 80 (2018).
6. Elbehiry, A. et al. Microbial food safety and antimicrobial resistance in foods: a dual threat to public health. *Microorganisms* **13** (7), 1592 (2025).
7. Nguyen, B. N., Peterson, B. N. & Portnoy, D. A. Listeriolysin O: a phagosome-specific Cytolysin revisited. *Cell. Microbiol.* **21**, e12988 (2019).
8. Xu, L. et al. Anti-inflammatory, antioxidant and anti-virulence roles of atractylodin in attenuating *Listeria monocytogenes* infection. *Front. Immunol.* **13**, 977051 (2022).
9. Lu, G. J., Xu, L., Zhang, T., Deng, X. M. & Wang, J. F. A potential bio-control agent from Baical skullcap root against listeriosis via the Inhibition of sortase A and Listeriolysin O. *J. Cell. Mol. Med.* **23**, 2042–2051 (2019).
10. Wang, J. F. et al. Fisetin inhibits *Listeria monocytogenes* virulence by interfering with the oligomerization of Listeriolysin O. *J. Infect. Dis.* **211**, 1376–1387 (2015).
11. Liu, M. D. et al. Isoflavone glucoside genistin, an inhibitor targeting sortase A and Listeriolysin O, attenuates the virulence of *Listeria monocytogenes in vivo* and *in vitro*. *Biochem. Pharmacol.* **209**, 115447 (2023).
12. Wang, J. F. et al. Phloretin attenuates *Listeria monocytogenes* virulence both *in vitro* and *in vivo* by simultaneously targeting listeriolysin O and sortase A. *Front. Cell. Infect. Microbiol.* **7**, 9 (2017).
13. Su, C. Y., Ming, Q. L., Rahman, K., Han, T. & Qin, L. P. *Salvia miltiorrhiza*: traditional medicinal uses, chemistry, and Pharmacology. *Chin. J. Nat. Med.* **13**, 163–182 (2015).
14. Tan, Y. L. et al. Tanshinone IIA promotes macrophage cholesterol efflux and attenuates atherosclerosis of apoE$^{-/-}$ mice by Omentin-1/ABCA1 pathway. *Curr. Pharm. Biotechnol.* **20**, 422–432 (2019).
15. Chang, C. C. et al. The anti-atherosclerotic effect of Tanshinone IIA is associated with the Inhibition of TNF-α-induced VCAM-1, ICAM-1 and CX3CL1 expression. *Phytomedicine* **21**, 207–216 (2014).
16. Fang, Z. Y. et al. Tanshinone IIA downregulates the CD40 expression and decreases MMP-2 activity on atherosclerosis induced by high fatty diet in rabbit. *J. Ethnopharmacol.* **115**, 217–222 (2008).
17. Fang, Z. Y. et al. Tanshinone IIA: A review of its anticancer effects. *Front. Pharmacol.* **11**, 611087 (2020).
18. Qian, J. et al. Tanshinone IIA alleviates the biological characteristics of colorectal cancer via activating the ROS/JNK signaling pathway. *Anti-Cancer Agents Med. Chem.* **23**, 227–236 (2023).
19. Guo, C. et al. Study on the antitumor mechanism of Tanshinone IIA *in vivo* and *in vitro* through the regulation of PERK-ATF4-HSPA5 pathway-mediated ferroptosis. *Molecules* **29**, 1557 (2024).
20. Shinhmar, S. et al. Developing a tanshinone IIA memetic by targeting MIOS to regulate mTORC1 and autophagy in glioblastoma. *Int. J. Mol. Sci.* **25**, 6586 (2024).
21. Yuan, L. M. et al. Tanshinone IIA inhibits the adipogenesis and inflammatory response in ox-LDL-challenged human monocyte-derived macrophages via regulating miR-130b/WNT5A. *J. Cell. Biochem.* **121**, 1400–1408 (2020).
22. Wang, X. et al. Tanshinone IIA protected against lipopolysaccharide-induced brain injury through the protective effect of the blood-brain barrier and the suppression of oxidant stress and inflammatory response. *Food Funct.* **13**, 8304–8312 (2022).
23. Li, Y. et al. Tanshinone IIA alleviates NLRP3 inflammasome-mediated pyroptosis in *Mycobacterium tuberculosis*-(H37Ra-) infected macrophages by inhibiting Endoplasmic reticulum stress. *J. Ethnopharmacol.* **282**, 114595 (2022).
24. Chen, H. et al. Tanshinone Iia inhibits megakaryopoiesis in immune vasculitis. *Blood* **138**, S4288 (2021).
25. Wang, Y. X. et al. Tanshinone IIA attenuates paraquat-induced acute lung injury by modulating angiotensin-converting enzyme 2/angiotensin-(1–7) in rats. *Mol. Med. Rep.* **18**, 2955–2962 (2018).
26. Fu, K. Q., Feng, C., Shao, L. Z., Mei, L. & Cao, R. F. Tanshinone IIA exhibits anti-inflammatory and antioxidative effects in LPS-stimulated bovine endometrial epithelial cells by activating the Nrf2 signaling pathway. *Res. Vet. Sci.* **136**, 220–226 (2021).
27. Osborne, S. E. & Brumell, J. H. Listeriolysin O: from bazooka to Swiss army knife. *Philos. Trans. R Soc. Lond. B Biol. Sci.* **372** (1726), 20160222 (2017).
28. Seveau, S. Multifaceted activity of Listeriolysin O, the cholesterol-dependent Cytolysin of *Listeria monocytogenes*. *Subcell. Biochem.* **80**, 161–195 (2014).
29. Kong, C., Neoh, H. M. & Nathan, S. Targeting *Staphylococcus aureus* toxins: a potential form of anti-virulence therapy. *Toxins* **8** (3), 72 (2016).
30. Drolia, R. & Bhunia, A. K. Crossing the intestinal barrier via *Listeria* adhesion protein and internalin A. *Trends Microbiol.* **27** (5), 408–425 (2019).

31. Eallonardo, S. J. & Freitag, N. E. Crossing the barrier: A comparative study of *Listeria monocytogenes* and *Treponema pallidum* in placental invasion. *Cells* **13** (1), 88 (2023).
32. Hamon, M. A., Ribet, D., Stavru, F. & Cossart, P. Listeriolysin O: the Swiss army knife of *Listeria*. *Trends Microbiol.* **20** (8), 360–368 (2012).
33. Tao, L., Wang, G. Y., Wang, M. Y., Chen, Y. L. & Fan, Z. Q. Study on acute toxicity and antiinflammation of Tanshinone extract. *Biol. Chem. Eng.* **8** (5), 90–92 (2022).
34. Su, C. C. & Chiu, T. L. Tanshinone IIA decreases the protein expression of EGFR, and IGFR blocking the PI3K/Akt/mTOR pathway in gastric carcinoma AGS cells both *in vitro* and *in vivo*. *Oncol. Rep.* **36**, 1173–1179 (2016).
35. Köster, S. et al. Crystal structure of Listeriolysin O reveals molecular details of oligomerization and pore formation. *Nat. Commun.* **5**, 3690 (2014).
36. Quereda, J. J. et al. Pathogenicity and virulence of *Listeria monocytogenes*: a trip from environmental to medical microbiology. *Virulence* **12**, 2509–2545 (2021).
37. Lecuit, M. *Listeria monocytogenes*, a model in infection biology. *Cell. Microbiol.* **22**, e13186 (2020).
38. Zou, Y. N. et al. Isorhamnetin as a novel inhibitor of pneumolysin against *Streptococcus pneumoniae* infection in vivo/in vitro. *Microb. Pathogenesis.* **185**, 106382 (2023).
39. Adasme, M. F. et al. PLIP 2021: expanding the scope of the protein-ligand interaction profiler to DNA and RNA. *Nucleic Acids Res.* **49**, W530–W534 (2021).
40. Wang, H. T., Hu, S. Y., Pei, Y. Z. & Sun, H. X. Nordalbergin synergizes with novel β-lactam antibiotics against MRSA infection. *Int. J. Mol. Sci.* **25**, 7704 (2024).

Acknowledgements
No.

Author contributions
H.W. and H.S. conceived and designed the experiments; H.W., S.H., and H.F. performed the experiments; H.W. and H.F. analyzed the data; H.W. and S.H. wrote the original draft paper. H.S revised and edited the manuscript. All authors have read and approved the final manuscript.

Funding
This work was supported by the Pioneer and Leading Goose R&D Program of Zhejiang (2023C02047), National Key R&D Program of China (2023YFD1800804) and the National Natural Science Foundation of China (32273059).

Declarations

Competing interests
The authors declare no competing interests.

Ethics approval
All animal experimental procedures were approved by the Jilin University Institutional Animal Care Committee (SY202309036).

Consent for publication
Not applicable.

Additional information
Supplementary Information The online version contains supplementary material available at https://doi.org/10.1038/s41598-025-19988-3.

Correspondence and requests for materials should be addressed to H.S.

Reprints and permissions information is available at www.nature.com/reprints.

Publisher's note Springer Nature remains neutral with regard to jurisdictional claims in published maps and institutional affiliations.